Impacts of Enhanced Weathering on biomass production for negative emission technologies and soil hydrology

Wagner de Oliveira Garcia*[1], Thorben Amann[1], Jens Hartmann[1], Kristine Karstens[2], Alexander Popp[2], Lena R. Boysen[3], Pete Smith[4], Daniel Goll[5,6]

[1]Institute for Geology, Center for Earth System Research and Sustainability, Universität Hamburg, Germany
[2]Potsdam Institute for Climate Impact Research (PIK), Germany
[3]Max Planck Institute for Meteorology, Germany
[4]Institute of Biological and Environmental Sciences, School of Biological Sciences, University of Aberdeen
[5]Laboratoire des Sciences du Climat et de l'Environnement, CEA CNRS UVSQ, 91190 Gif-sur-Yvette, France
[6]Institute of Geography, University Augsburg, Germany

**Correspondense to*: Wagner de Oliveira Garcia (wagner.o.garcia@gmail.com) ORCID: https://orcid.org/0000-0001-9559-0629

Supplementary information

Summary

Abbreviation

Mg, Ca, K, P	Macronutrients, respectively: Magnesium, Calcium, Potassium, Phosphorus	
RCP4.5	Representative Concentration Pathway for radiative forcing value in 2100 of +4.5 W m^{-2} relative to pre-industrial values.	
AR	Afforestation/Reforestation	
BECCS	Bio-Energy with Carbon Capture and Storage	
PTF	Pedotransfer Functions	
Fine basalt powder	Basalt powder texture of 15.6% clay, 83.8% silt and 0.6% fine sand	
Coarse basalt powder	Basalt powder texture of 15.6% clay, 53.8% silt and 30.6% fine sand	
S	Sand texture	[wt %]
C	Clay texture	[wt %]
OM	Soil organic matter	[wt %]
θ_{1500} and θ_{33} [a]	Moisture for a pressure head of -1500 kPa and of -33 kPa.	[wt %]
$\theta_{(S-33)}$ [a]	0 kPa to -33 kPa moisture	[wt %]
θ_S [a]	Saturated (0 kPa) moisture	[wt %]
K_S [a]	Saturated soil hydraulic conductivity	[mm h^{-1}]
λ [a]	Slope of logarithmic tension-moisture curve	[-]
G_{cor}	Corrected soil texture after basalt application	[-]
G_{ini}	Initial soil texture	[-]
V_{cell}	Raster cell volume	[km^3]
ρ_{bulk_cell}	Soil bulk density	[$kg.km^{-3}$]
M_{soil_cell}	Total sediment mass	[kg]
OM_c	Corrected organic matter content	[wt %]
OM_{cell}	Organic matter mass	[kg]
M_{b_cell}	Basalt mass	[kg]
M_{soil_cell}	Soil mass	[kg]
G_{basalt}	Basalt texture	[-]
G_{bs}	Texture fractions of resulting mixture of basalt plus soil	[-]

[a] equation from (Saxton and Rawls, 2006).

A. Introduction

The stoichiometric ratios used to estimate the median and ranges (5th and 95th percentiles) macronutrient demand by afforestation in the main text section "Nutrient demand Afforestation/Reforestation" are presented as an excel file "S2.xlsx". In the chapter B, we present the results that were not presented in main text for EW coupled with AR that are: the potential P gaps and the necessary basalt powder deployment to bridge the estimated P gaps for an N-limited AR scenario and the related C-fixation reduction (Fig. S 1, Fig. S2, Fig. S 3, and Fig. S4) and the potential P gaps and the necessary basalt powder deployment to bridge the estimated P gaps for an N-unlimited AR scenario and the related C-fixation reduction (Fig. S 5, Fig. S6 , Fig. S 7, Fig. S8, Fig. S 9, and Fig. S10). In chapter C, we show the results for a hypothetical scenario assuming that the estimated maximum harvest rate by MAgPIE could be increased by one order of magnitude (Fig. S 11). The soil hydrology impacts for a coarse and for a fine rock powder texture is presented in chapter D for the P budget of geogenic P supply scenario two for the N-unlimited scenario, the impacts on soil hydraulic conductivity and plant available water could be neglected (Fig. S 12). The results for impacts in soil hydrology are presented for the N-unlimited AR scenario, since the required amount of rock powder to bridge the projected P gaps will be higher than for an N-limited scenario. Consequently, the changes in soil hydraulic properties for the N-unlimited AR scenario will be more remarkable than for the N-limited AR-scenario.

B. EW coupled with AR

i. AR N-limited

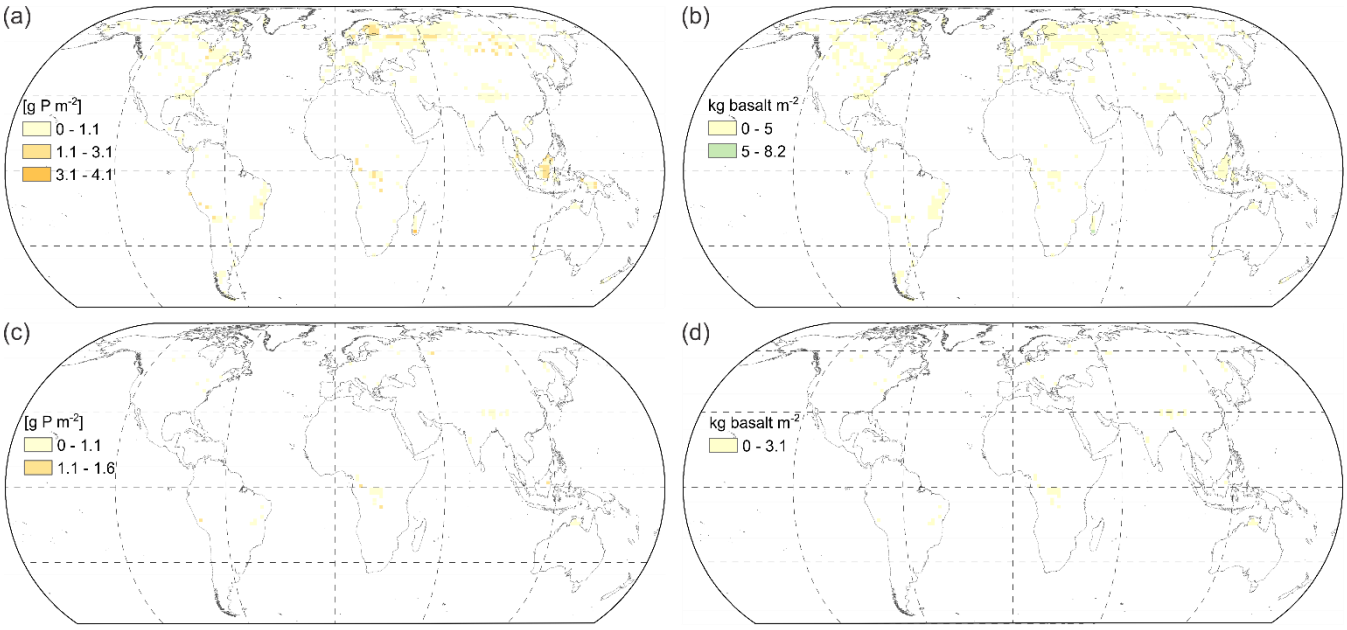

Fig. S 1: Areas with potential P gap for the nutrient budget of the N-limited AR scenario (after 94 years of simulation) assuming P concentrations within foliar and wood material corresponding to 5th percentile values (main text Table 1). a) Geogenic P supply scenario one (geogenic P from weathering plus atmospheric P deposition as source of P). b) Basalt deployment necessary to close P gaps from P budget scenario of Fig. S 1a. c) Geogenic P supply scenario two (geogenic P from soil inorganic labile P and organic P pools plus atmospheric P deposition and P from weathering as source of P). d) Basalt deployment necessary to close P gaps from P budget scenario of Fig. S 1c. Map generated with ESRI ArcGIS 10.7 (http://www.esri.com).

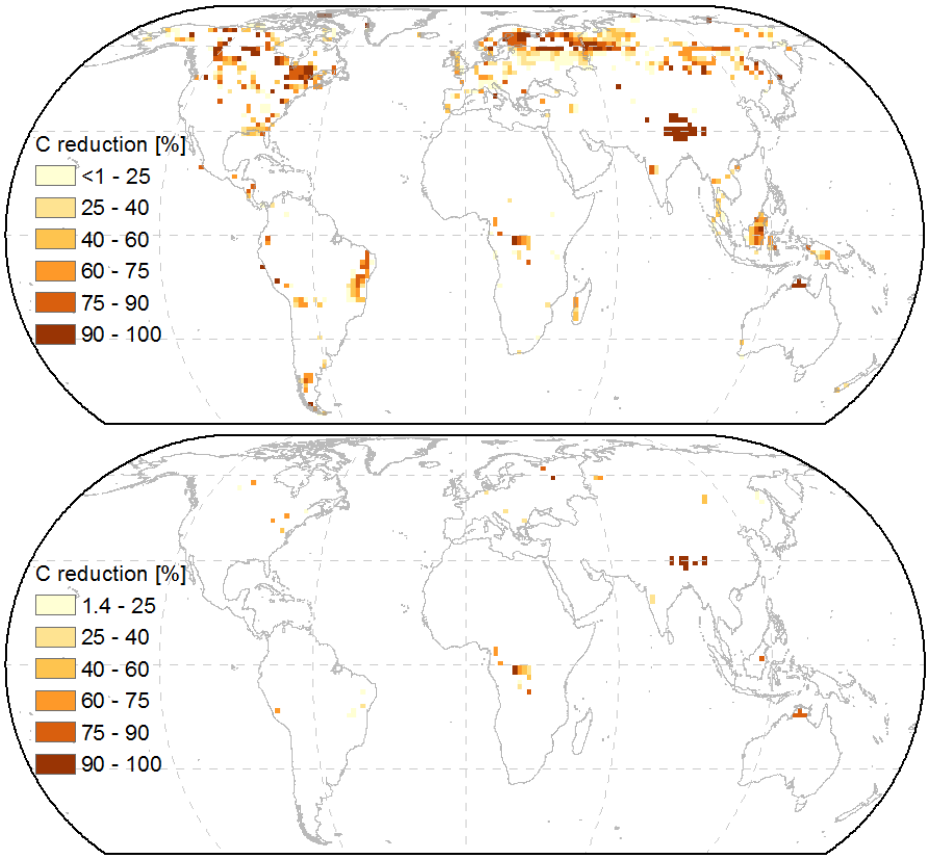

Fig. S2: Forest C sequestration reduction due to geogenic P limitation assuming P concentrations within foliar and wood material corresponding to 5th values (main text Table 1) estimated from stoichiometric C:P ratios. a) C-reduction based on P gaps of Fig. S 1a, obtained for geogenic P supply scenario one (geogenic P from weathering plus atmospheric P deposition as source of P). b) C-reduction based on P gaps of Fig. S 1c, obtained for geogenic P supply scenario two (geogenic P from soil inorganic labile P and organic P pools plus atmospheric P deposition and P from weathering as source of P). Map generated with ESRI ArcGIS 10.7 (*http://www.esri.com*).

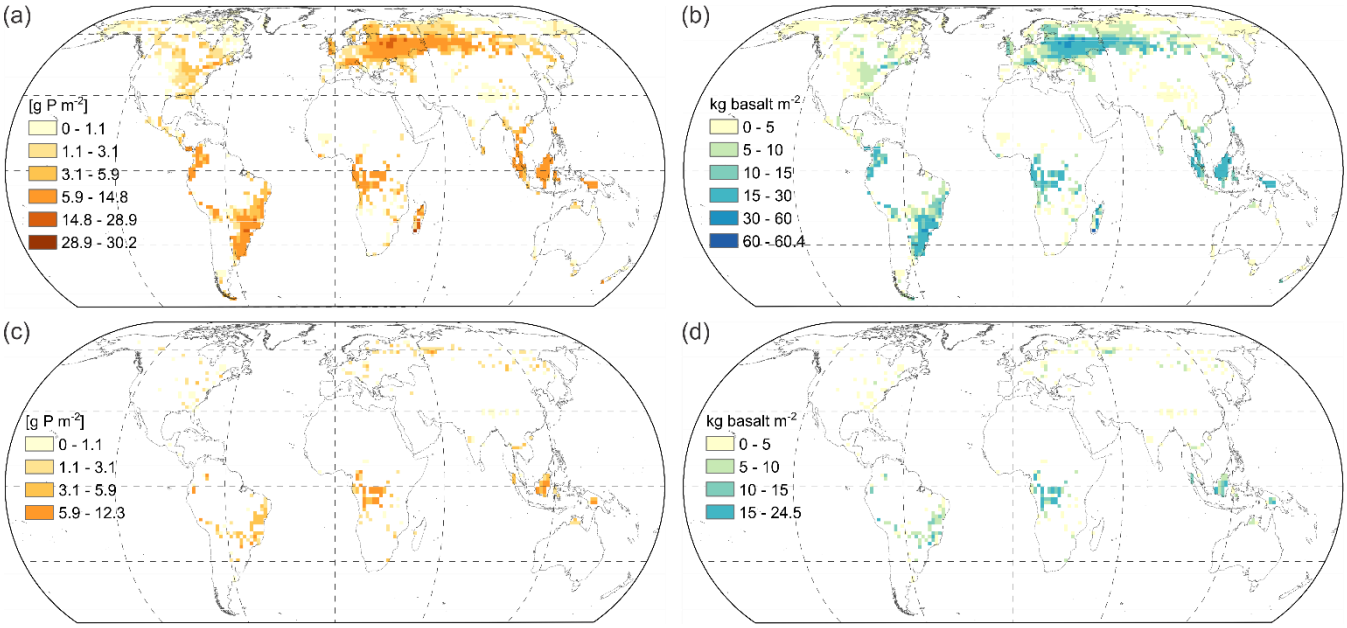

Fig. S 3: Areas with potential P gap for the nutrient budget of the N-limited AR scenario (after 94 years of simulation) assuming P concentrations within foliar and wood material corresponding to 95th percentile values (main text Table 1). a) Geogenic P supply scenario one (geogenic P from weathering plus atmospheric P deposition as source of P). b) Basalt deployment necessary to close P gaps from P budget scenario of Fig. S 3a. c) Geogenic P supply scenario two (geogenic P from soil inorganic labile P and organic P pools plus atmospheric P deposition and P from weathering as source of P). d) Basalt deployment necessary to close P gaps from P budget scenario of Fig. S 3c. Map generated with ESRI ArcGIS 10.7 (http://www.esri.com).

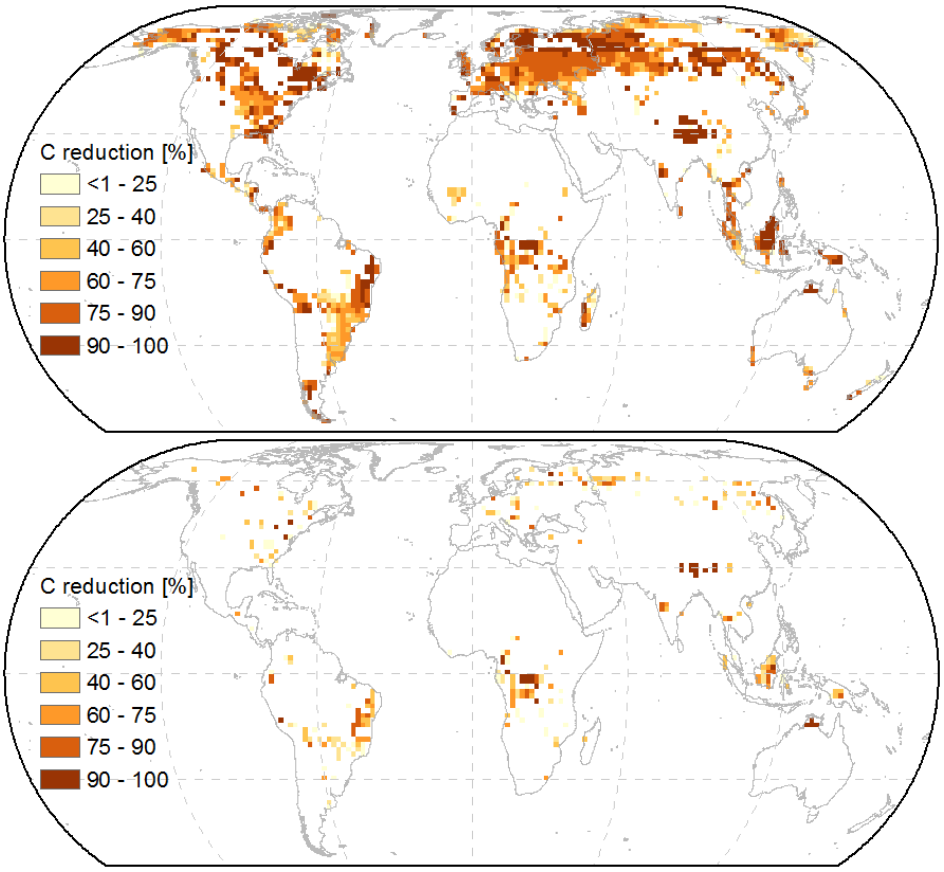

Fig. S4: Forest C sequestration reduction due to geogenic P limitation assuming P concentrations within foliar and wood material corresponding to 95th values (main text Table 1) estimated from stoichiometric C:P ratios. a) C-reduction based on P gaps of Fig. S 3a, obtained for geogenic P supply scenario one (geogenic P from weathering plus atmospheric P deposition as source of P). b) C-reduction based on P gaps of Fig. S 3c, obtained for geogenic P supply scenario two (geogenic P from soil inorganic labile P and organic P pools plus atmospheric P deposition and P from weathering as source of P). Map generated with ESRI ArcGIS 10.7 (*http://www.esri.com*).

ii. AR N-unlimited

The predicted C sequestration by N-unlimited AR scenario from Kracher (2017) is ~2.4 Gt C a^{-1}. Different authors reported the potential C sequestration by afforestation or reforestation being of 0.3 – 3.3 Gt C a^{-1} for the end of 2100 (National Research Council, 2015;Lenton, 2014, 2010;Smith et al., 2015 apud Fuss et al., 2018). However, the predicted sequestration potential estimated by Kracher (2017) can fall to ~1.4 Gt C a^{-1} if geogenic P supply scenario one for mean P content within wood and leaves is selected. If geogenic P supply scenario two for mean P content within wood and leaves is selected, it fall to ~2.2 Gt C a^{-1}.

The ideal P biomass additional demand (calculated from main text Eq. (1)), to sequester 224 Gt C (N-unlimited AR scenario) amounts to 244 Mt P on global scale for a mean wood and leaves P content; for 5th and 95th percentile, the estimated P demand would be 88 and 417 Mt P respectively. The potential C sequestration and the P demand of the N-unlimited AR scenario is higher than for the N-limited AR scenario.

The P budget for geogenic P supply scenario one, which considers P supply by weathering and atmospheric P deposition, for both N supply AR scenarios suggest that P deficiency areas are distributed along the world, but with higher occurrence within the northern hemisphere (Fig. S 7a). However, for geogenic P supply scenario two, which is the same as geogenic P supply scenario one plus geogenic P from soil inorganic labile P and organic P pools, the P deficiency areas are predominantly located at the southern hemisphere for both N supply AR scenarios (Fig. S 7c). If P is the only limiting nutrient, it is expected a C reduction of 1.8 – 52% from the projected 224 Gt C, with mean C reduction of 39% for the geogenic P supply scenario one

and 6% for the geogenic P supply scenario two (Table S2). If N and P are limiting nutrients, it is expected a C reduction of 16.5 – 59%, with mean C reduction of 47% for the geogenic P supply scenario one and 19% for the geogenic P supply scenario two. Accounting for N and P limitation on AR suggests that, in average; the biomass production will be affected, which decreases the C sequestration potential of AR strategies (Table S2). In some areas, the C sequestration reduction can reach up to 100% from predicted C sequestration of the AR models (Fig. S8).

Assuming a median P content of 500 ppm in basalt, the maximum mass applied in 94 years would be of 34 and 13 kg basalt m^{-2} respectively for P gap from geogenic P supply scenarios one and two for the N-unlimited AR scenario and mean P concentrations within foliar and wood material (Fig. S 7). A total amount of 3.6 – 454 Gt basalt (N-unlimited AR scenario) applied by EW would be needed to cover the projected P gaps. To reach the maximum projected C sequestration potential of AR, covering the N and P biomass demand would be necessary. Basalt has a carbon capture potential of ~0.3 $tCO_2\ t^{-1}$ basalt (Renforth, 2012), sequestering ~0.3 – ~37 Gt C (~1 – ~136.2 Gt CO_2) by the end of 2100 if basalt powder would be deployed to cover P gaps of the N-unlimited AR scenario.

The nutrient concentration of rocks will influence the necessary amounts to cover P gap of each P budget scenario for the AR scenarios. The cumulative applied rock powder mass will be different for each rock type (Table S1), with basalt being more effective to supply P for the estimated P gap areas due to relative high P content.

For a chemical composition corresponding to the 95th percentile, 10 kg basalt m^{-2} would cover the maximum projected P gaps for all P supply scenarios. For a median chemical composition, deploying 34 kg basalt m^{-2} would cover all the P gaps of the two geogenic P supply scenarios for the N-unlimited AR scenario and for the 5th percentile the necessary amount of rock would get even higher (Table S1).

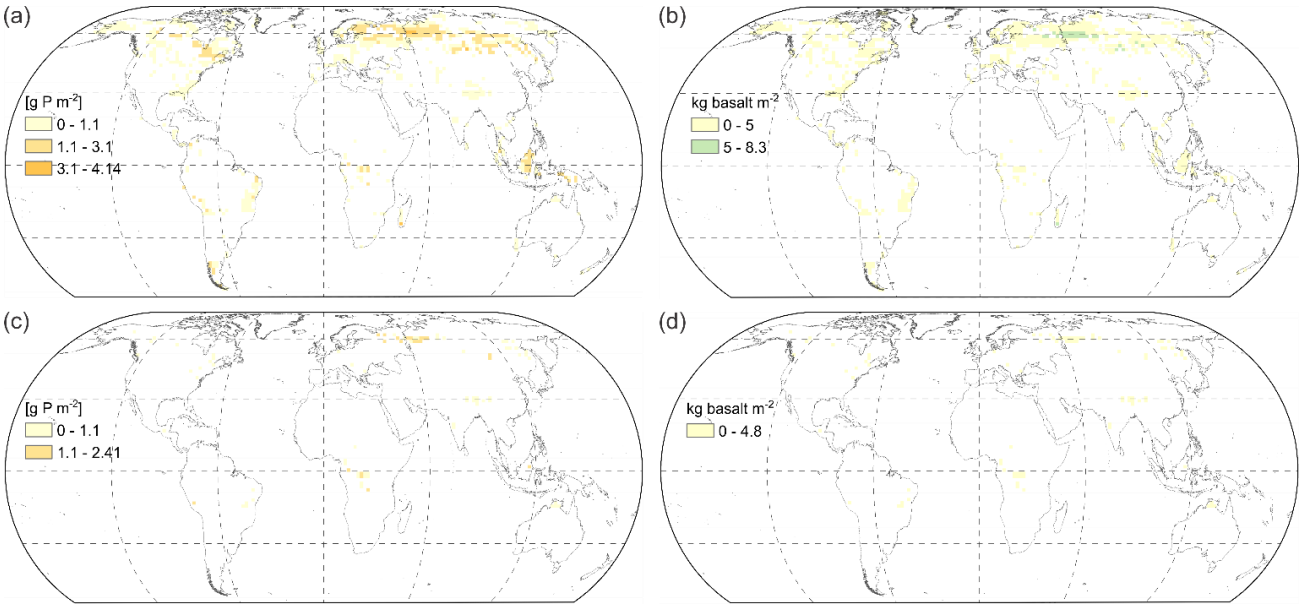

Fig. S 5: Areas with potential P gap for the nutrient budget of the N-unlimited AR scenario (after 94 years of simulation) assuming P concentrations within foliar and wood material corresponding to 5th percentile values (main text Table 1). a) Geogenic P supply scenario one (geogenic P from weathering plus atmospheric P deposition as source of P). b) Basalt deployment necessary to close P gaps from P budget scenario of Fig. S 5a. c) Geogenic P supply scenario two (geogenic P from soil inorganic labile P and organic P pools plus atmospheric P deposition and P from weathering as source of P). d) Basalt deployment necessary to close P gaps from P budget scenario of Fig. S 5c. Map generated with ESRI ArcGIS 10.7 (http://www.esri.com).

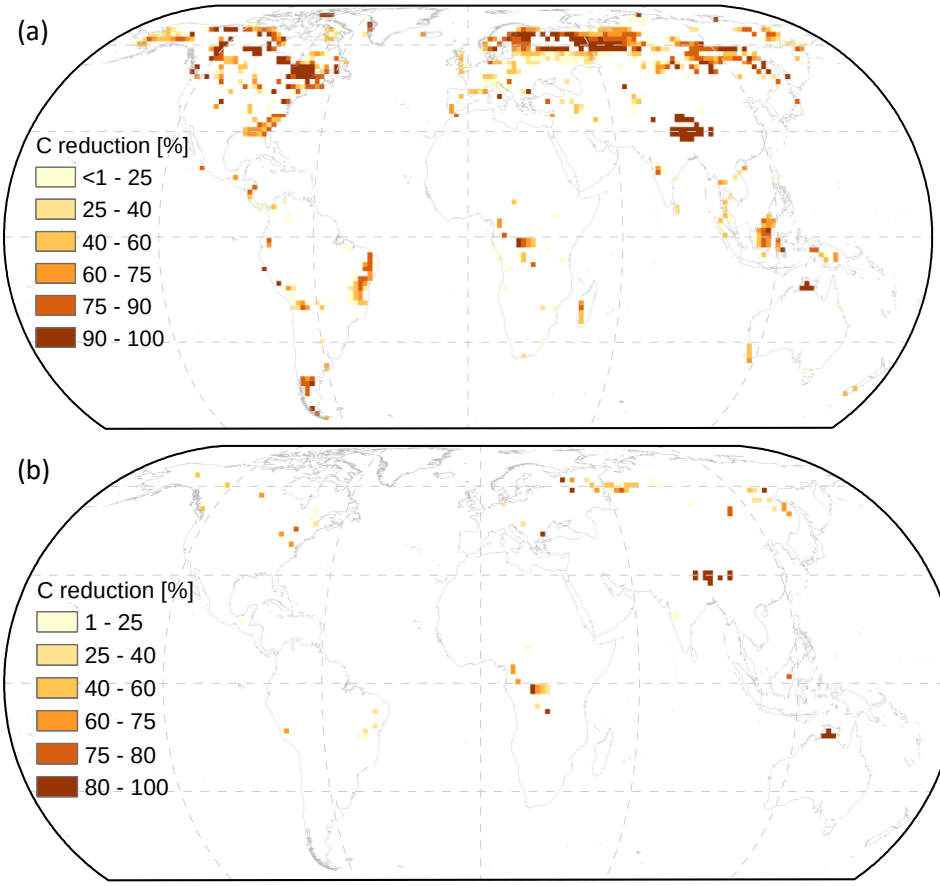

Fig. S6: Forest C sequestration reduction due to geogenic P limitation assuming P concentrations within foliar and wood material corresponding to 5th values (main text Table 1) estimated from stoichiometric C:P ratios. a) C-reduction based on P gaps of Fig. S 5a, obtained for geogenic P supply scenario one (geogenic P from weathering plus atmospheric P deposition as source of P). b) C-reduction based on P gaps of Fig. S 5c, obtained for geogenic P supply scenario two (geogenic P from soil inorganic labile P and organic P pools plus atmospheric P deposition and P from weathering as source of P). Map generated with ESRI ArcGIS 10.7 (*http://www.esri.com*).

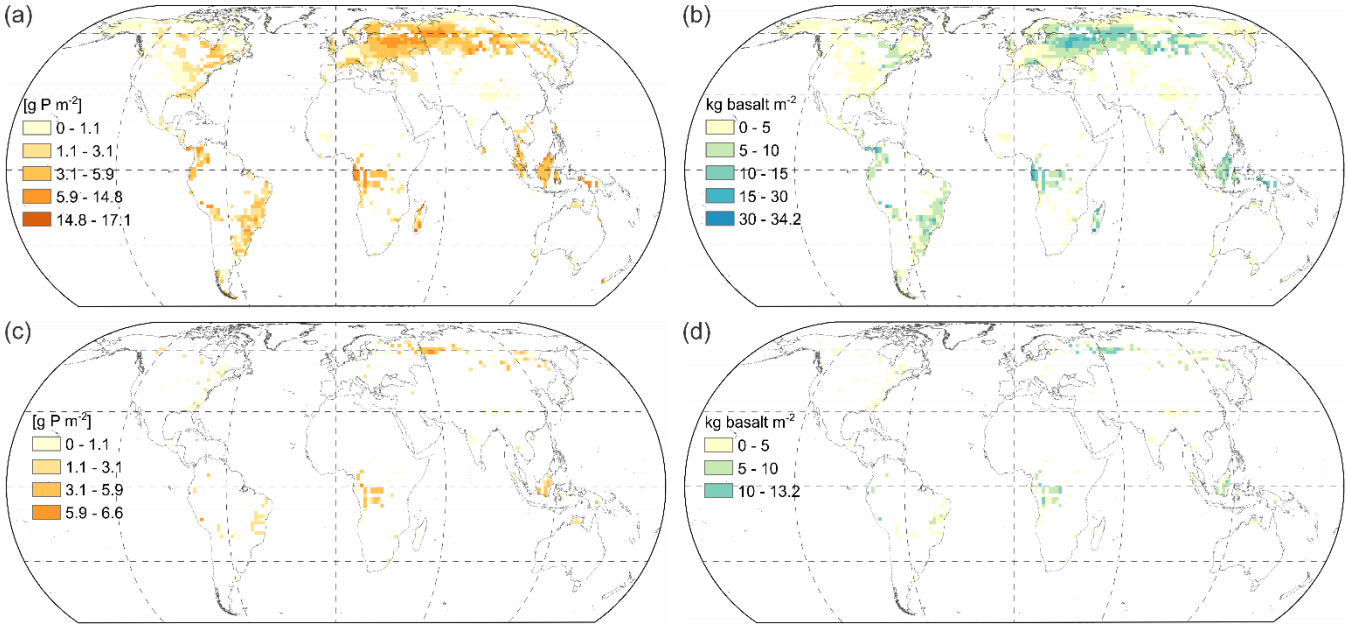

Fig. S 7: Areas with potential P gap for the nutrient budget of the N-unlimited AR scenario (after 94 years of simulation) assuming P concentrations within foliar and wood material corresponding to mean values (main text Table 1). a) Geogenic P supply scenario one (geogenic P from weathering plus atmospheric P deposition as source of P). b) Basalt deployment necessary to close P gaps from P budget scenario of Fig. S 7a. c) Geogenic P supply scenario two (geogenic P from soil inorganic labile P and organic P pools plus atmospheric P deposition and P from weathering as source of P). d) Basalt deployment necessary to close P gaps from P budget scenario of Fig. S 7c. Map generated with ESRI ArcGIS 10.7 (http://www.esri.com).

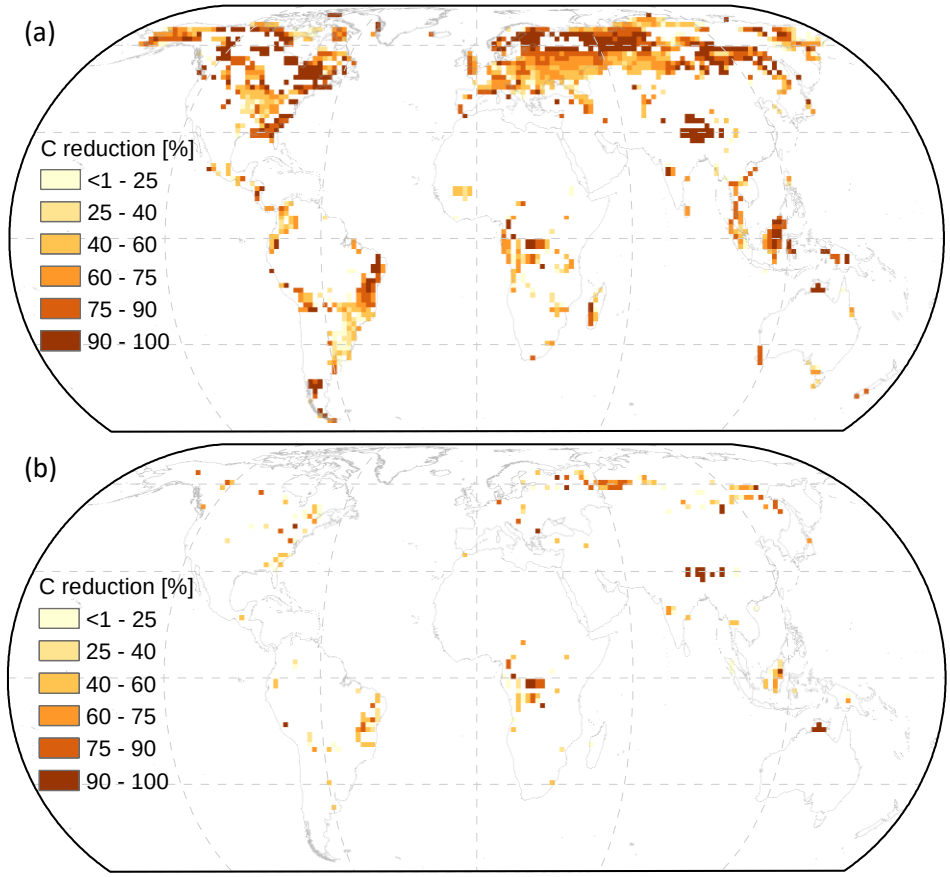

Fig. S8: Reduction on forest C sequestration due to geogenic P limitation. C-reduction estimated from stoichiometric C:P ratios for the N-unlimited AR scenario assuming P concentrations within foliar and wood material corresponding to mean values (Table 1 main text). a) C-reduction based on P gaps of Fig. S 7a, obtained for geogenic P supply scenario one (geogenic P from weathering plus atmospheric P deposition as source of P). b) C-reduction based on P gaps of Fig. S 7c, obtained for geogenic P supply scenario two (geogenic P from soil inorganic labile P and organic P pools plus atmospheric P deposition and P from weathering as source of P). For resulting global C reduction check Table S2. Map generated with ESRI ArcGIS 10.7 (http://www.esri.com).

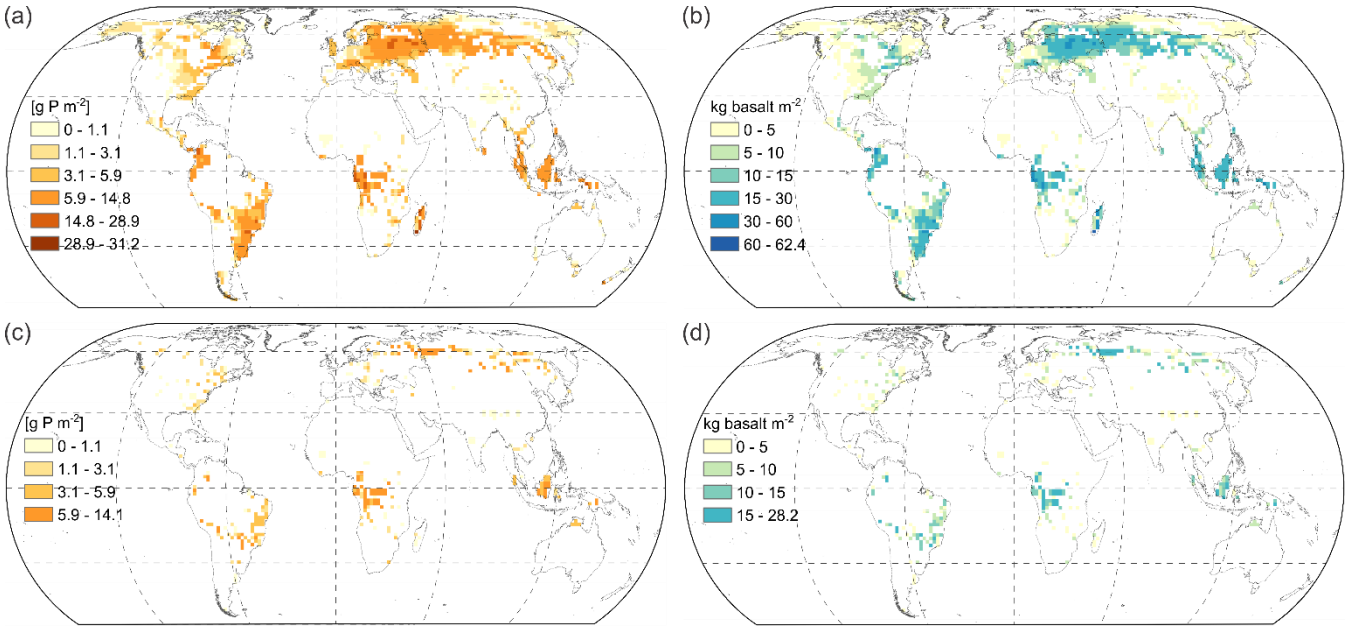

Fig. S 9: Areas with potential P gap for the nutrient budget of the N-unlimited AR scenario (after 94 years of simulation) assuming P concentrations within foliar and wood material corresponding to 95th percentile values (main text Table 1). a) Geogenic P supply scenario one (geogenic P from weathering plus atmospheric P deposition as source of P). b) Basalt deployment necessary to close P gaps from P budget scenario of Fig. S 9a. c) Geogenic P supply scenario two (geogenic P from soil inorganic labile P and organic P pools plus atmospheric P deposition and P from weathering as source of P). d) Basalt deployment necessary to close P gaps from P budget scenario of Fig. S 9c. Map generated with ESRI ArcGIS 10.7 (http://www.esri.com).

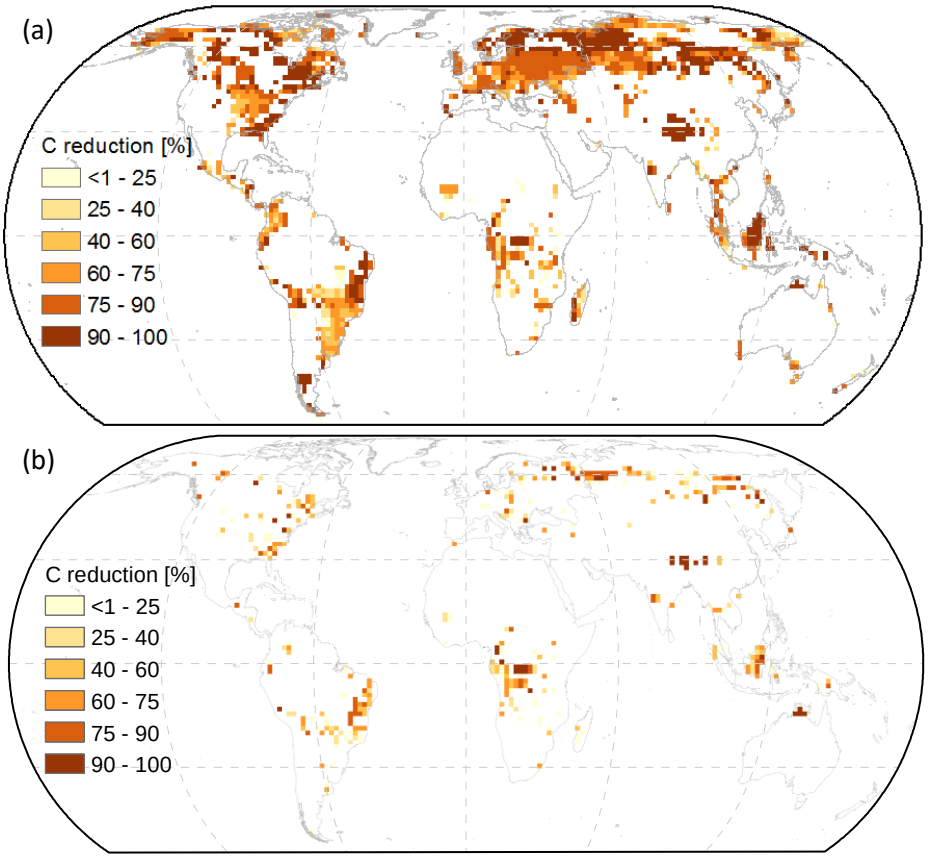

Fig. S10: Forest C sequestration reduction due to geogenic P limitation assuming P concentrations within foliar and wood material corresponding to 95th values (main text Table 1) estimated from stoichiometric C:P ratios. a) C-reduction based on P gaps of Fig. S 9a, obtained for geogenic P supply scenario one (geogenic P from weathering plus atmospheric P deposition as source of P). b) C-reduction based on P gaps of Fig. S 9c, obtained for geogenic P supply scenario two (geogenic P from soil inorganic labile P and organic P pools plus atmospheric P deposition and P from weathering as source of P). Map generated with ESRI ArcGIS 10.7 (*http://www.esri.com*).

Table S1: Rock powder application for a chemistry corresponding to the 5th percentile, assuming full rock dissolution, to cover maximum and median estimated P gaps for the N-unlimited AR scenario (minimum values can be neglected). For the potential macronutrient supply, see Fig. 7 main text and Fig. S 7.

	P gap [g P m^{-2}]	Rhyolite	Dacite	Andesite	Basalt
		[kg rock m^{-2}]			
Scenario one	17.1	783.4	156.7	120.5	112.0
	2.1	19.0	6.3	6.0	3.8
Scenario two	6.6	302.6	60.5	46.5	43.2
	1.8	17.0	5.7	5.3	3.4

Table S2: Global P gap, maximum estimated P gap, maximum C sequestration reduction, and global C reduction for the natural N supply (N-limited) AR scenario (projected C sequestration of 190 Gt C) and for the N fertilization (N-unlimited) AR scenario (projected C sequestration of 224 Gt C).

N supply	Geogenic P supply	Maximum estimated P gap [g P m^{-2}]			Global P gap [Mt P]			Maximum C sequestration reduction [kg C m^{-2}]			Global C reduction [Gt C]		
		Wood and leaves P content											
		5th percentile	mean	95th percentile	5th percentile	mean	95th percentile	5th percentile	mean	95th percentile	5th percentile	mean	95th percentile
Unlimited	Scenario one	4.1	17.1	31.2	16.0	100.0	227.0	10.0	15.0	16.0	34.0	88.0	117.0
	Scenario two	2.4	6.6	14.1	1.8	15.0	49.0	4.6	6.1	7.6	4.0	13.0	25.0

C. EW coupled to bio-energy grass production

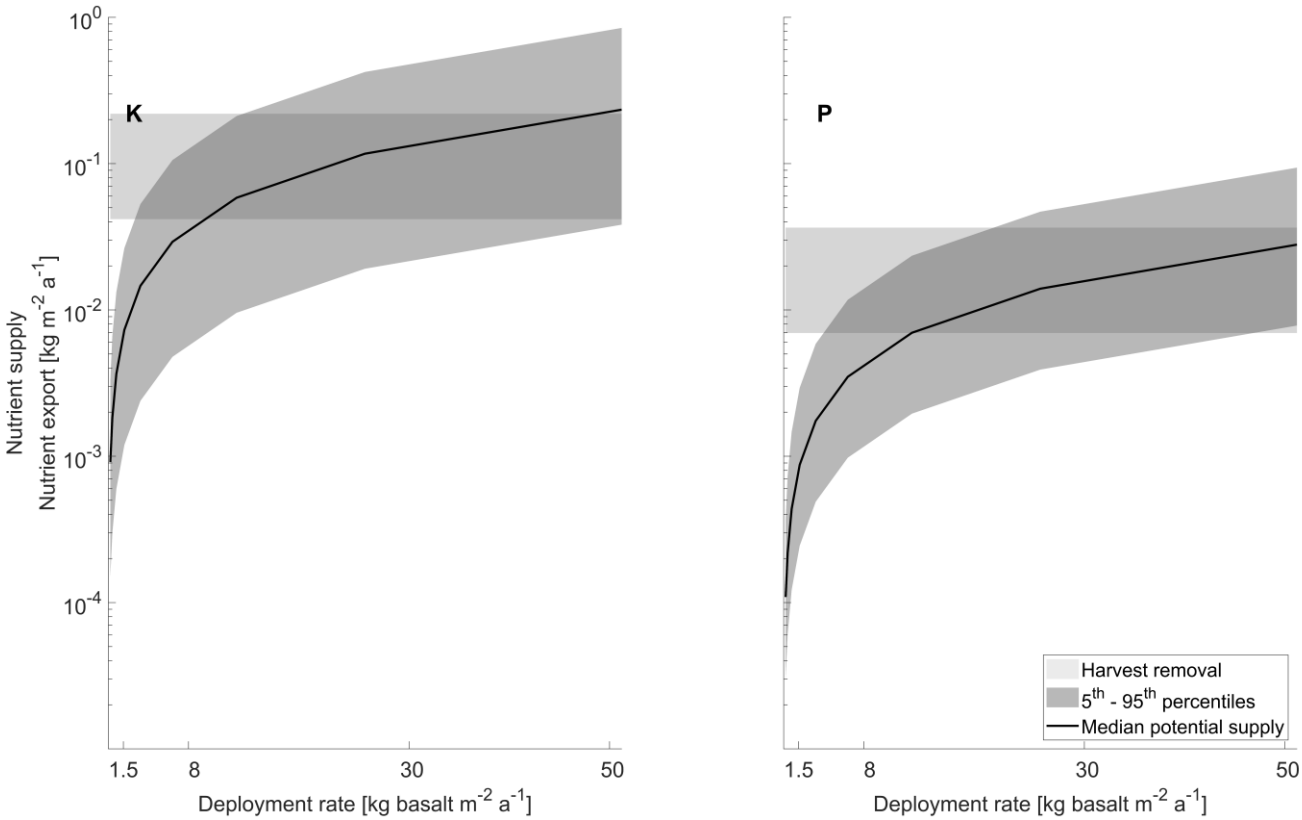

Fig. S 11: Projected K and P supply (logarithmic curve) by basalt complete dissolution given as median ranges (5th and 95th percentiles) for bio-energy grasses K and P demand (horizontal filled boxes) based on global minimum 0.7 kg m^{-2} a^{-1} and maximum 36 kg m^{-2} a^{-1} harvest rates.

D. Impacts on soil hydrology

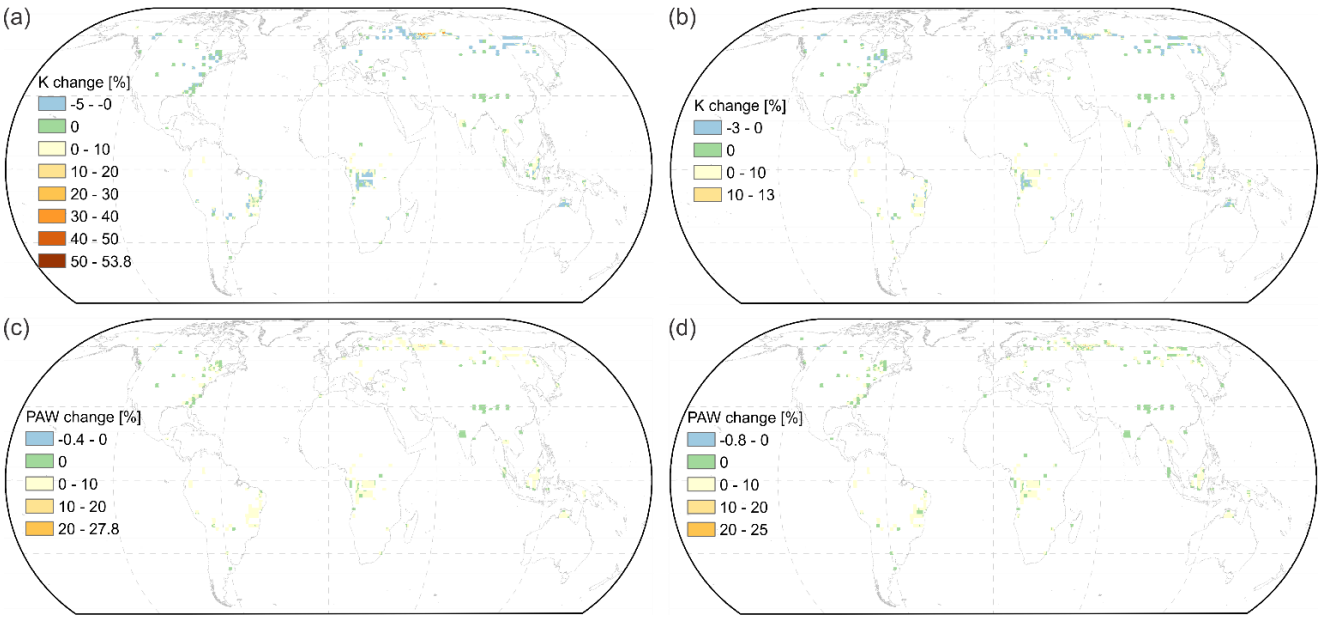

Fig. S 12: Impacts on soil hydrology estimated according to Saxton and Rawls (2006) equations for basalt deployment mass coincident to areas with potential P gap for the nutrient budget of the N-unlimited AR scenario assuming P concentrations within foliar and wood material corresponding to mean values (Fig. S 7c). a) Hydraulic conductivity (K) changes relative to initial soil

values for a fine basalt texture (15.6% clay, 83.8% silt, and 0.6% sand) being deployed. b) Hydraulic conductivity (K) changes relative to initial soil values for a coarse basalt texture (15.6% clay, 53.8% silt, and 30.6% fine sand) being deployed. c) Plant available water (PAW) changes relative to initial soil values for a fine basalt texture being deployed. d) Plant available water (PAW) changes relative to initial soil values for a coarse basalt texture being deployed. Map generated with ESRI ArcGIS 10.7 (http://www.esri.com).

E. References

Council, N. R.: Climate Intervention: Carbon Dioxide Removal and Reliable Sequestration, The National Academies Press, Washington, DC, 154 pp., 2015.

Kracher, D.: Nitrogen-Related Constraints of Carbon Uptake by Large-Scale Forest Expansion: Simulation Study for Climate Change and Management Scenarios, Earth's Future, 5, 1102-1118, 10.1002/2017EF000622, 2017.

Lenton, T. M.: The potential for land-based biological CO2 removal to lower future atmospheric CO2 concentration, Carbon Management, 1, 145-160, 2010.

Lenton, T. M.: The global potential for carbon dioxide removal, Geoengineering of the Climate System, 52-79, 2014.

Renforth, P.: The potential of enhanced weathering in the UK, International Journal of Greenhouse Gas Control, 10, 229-243, 10.1016/j.ijggc.2012.06.011, 2012.

Saxton, K. E., and Rawls, W. J.: Soil water characteristic estimates by texture and organic matter for hydrologic solutions, Soil science society of America Journal, 70, 1569-1578, 2006.

Smith, P., Davis, S. J., Creutzig, F., Fuss, S., Minx, J., Gabrielle, B., Kato, E., Jackson, R. B., Cowie, A., Kriegler, E., van Vuuren, D. P., Rogelj, J., Ciais, P., Milne, J., Canadell, J. G., McCollum, D., Peters, G., Andrew, R., Krey, V., Shrestha, G., Friedlingstein, P., Gasser, T., Grübler, A., Heidug, W. K., Jonas, M., Jones, C. D., Kraxner, F., Littleton, E., Lowe, J., Moreira, J. R., Nakicenovic, N., Obersteiner, M., Patwardhan, A., Rogner, M., Rubin, E., Sharifi, A., Torvanger, A., Yamagata, Y., Edmonds, J., and Yongsung, C.: Biophysical and economic limits to negative CO2 emissions, Nature Climate Change, 6, 42, 10.1038/nclimate2870

https://www.nature.com/articles/nclimate2870#supplementary-information, 2015.